JUNE 1980 PPPL-1668
UC-20c,d
LA-1424
CONF-800455--16

IMPURITY CONTROL IN TFTR

BY

J. L. CECCHI

PLASMA PHYSICS LABORATORY

PRINCETON UNIVERSITY
PRINCETON, NEW JERSEY

This work was supported by the U.S. Department of Energy Contract No. DE-AC02-76-CH0 3073. Reproduction, translation, publication, use and disposal, in whole or in part, by or for the United States government is permitted.

IMPURITY CONTROL IN TFTR

J. L. Cecchi

Plasma Physics Laboratory, Princeton University

Princeton, New Jersey, USA 08544

ABSTRACT

The control of impurities in TFTR will be a particularly difficult problem due to the large energy and particle fluxes expected in the device. As part of the TFTR Flexibility Modification (TFM) project, a program has been implemented to address this problem. Transport code simulations are used to infer an impurity limit criterion as a function of the impurity atomic number. The configurational designs of the limiters and associated protective plates are discussed along with the consideration of thermal and mechanical loads due to normal plasma operation, neutral beams, and plasma disruptions. A summary is given of the materials-related research, which has been a collaborative effort involving groups at Argonne National Laboratory, Sandia Laboratories, and Princeton Plasma Physics Laboratory. Conceptual designs are shown for gettering systems capable of regenerating absorbed tritium. Research on this topic by groups at the previously mentioned laboratories and SAES Research Laboratory is reviewed.

I Introduction

The Tokamak Fusion Test Reactor [1] (TFTR), presently under construction and scheduled for initial operation in late 1981, belongs to the next generation of magnetic confinement devices which are intended to investigate reactor-like operating regimes and further the development of associated fusion technology. The major components of TFTR are shown in Fig. 1. The vacuum vessel has a 2.65m major radius and a 1.1m minor radius. It is composed of 304LN stainless steel sections and Inconel 625 bellows assemblies. The maximum toroidal magnetic field is 5.2T at the plasma center (2.48m), and the main source of heating is neutral beam injection. The device will operate with both deuterium and tritium to exploit the large D-T fusion cross section for neutron and alpha particle production. One of the major objectives of TFTR is to maximize the fusion power gain.

To enhance the machine capabilities beyond those of the original design, the TFTR Flexibility Modification (TFM) project [2] was undertaken. The associated improvements are scheduled to be fully operational by mid-1983. One aspect of this project is an increase in the neutral beam power and pulse length. In the full TFM mode, four injection beam lines will provide a total neutral deuterium power of ~ 33.5MW for 1.5s. The 120 keV full energy component will carry ~ 75% of the total power. Along with this is an increase in the equilibrium magnetic field capability to 0.5T.

The projected plasma performance with the full neutral beam power is summarized in Table I from the results of the Baldur transport code [3]. In addition to the input parameters listed, the code assumes an electron thermal conductivity $\chi_e = 5 \times 10^{17}/n_e$ $cm^2 s^{-1}$, with n_e the electron density (cm^{-3}). Also, sufficient particle influx is included to produce the average electron

density $\langle n_e \rangle = 8 \times 10^{13} cm^{-3}$. Based upon the optimistic assumption of no impurities being present, the peak temperatures for ions and electrons are 22 keV and 14 keV, respectively. The corresponding fusion power gain Q is 2.5 and β, the ratio of plasma pressure to total magnetic field pressure, is 0.03. The addition of 0.5% Fe to this plasma, however, results in dramatic decreases in these parameters, including a 20% fractional reduction in β and a 40% fractional reduction in Q. It is clear that impurities constitute a formidable barrier to realizing the full operating potential of TFTR, and are especially deleterious to achieving maximum values of Q. Furthermore, the control of impurities in this device will be a particularly difficult problem, due to the large particle and energy fluxes which are expected in the TFM mode.

In consideration of this, an extensive impurity control program has been undertaken as part of the TFM project. Two closely related areas upon which this program has focused are the optimization of the limiter configuration and the selection of the most favorable materials on the basis of bulk thermal properties, surface properties, and tritium retention characteristics. These aspects are discussed in Section III and Section IV, respectively, following the presentation in Section II of a simple model for comparing the effects of impurities of different atomic numbers. Another major involvement of the impurity control program is the design of a gettering system compatible with TFM operation, including the limitations on the stored tritium inventory. This topic is presented in Section V. A discussion of the implications of the present work for the following generation of machines is given in Section VI. Besides the particular impurity control methods discussed here, considerable attention is also being devoted to the techniques for proper wall conditioning, including glow and pulse discharge cleaning. This subject is

reviewed elsewhere by Dylla [4]. A comprehensive presentation of the general topic of plasma-surface interactions is given by McCracken and Stott [5].

The materials and getter research have been a collaborative effort involving groups at Argonne National Laboratory, Sandia Laboratories, SAES Research Laboratory, and the Princeton Plasma Physics Laboratory.

II Impurity Concentration Limits

The presence of plasma impurities impacts the fusion power gain Q in two major respects. Firstly, the radiative losses which attend impurities and which increase strongly with atomic number Z will reduce plasma temperatures, and, consequently, β and Q. Based upon parametric studies with the Baldur code, Singer [3] has shown that for an impurity density n_I such that

$$\frac{\dot{n}_I}{n_e} < \frac{10}{Z^3} , \tag{1}$$

the associated fractional reduction in β is small, being typically less than 5%. This would imply a Q reduction of less than ~ 10%.

Besides adding to the radiative losses, impurities also cause a reduction in the deutrium tritium densities for fixed electron densities. From charge neutrality we have

$$n_e = n_i + Zn_I , \tag{2}$$

where $n_i \equiv n_D + n_T$, with n_D and n_T the deuterium and tritium densities, respectively. For a given ratio of n_D/n_T, the fusion power output in the TFM mode is proportional to n_i^2 which, from Eq. 2, is

$$n_i^2 = n_e^2 \left(1 - Z \frac{n_I}{n_e}\right)^2 . \qquad (3)$$

Thus the deutrium/tritium depletion reduces Q by the factor $(1 - Zn_I/n_e)^2$. If we invoke a criterion that this factor be greater than 0.9, which roughly corresponds to the limit implicit in Eq. 1, then as far as the depletion is concerned, the impurity fraction is bounded by,

$$\frac{n_I}{n_e} < \frac{0.05}{Z} . \qquad (4)$$

The limits from Eqs. 1 and 4 are plotted in Fig. 2. For impurities with $Z < 14$, the depletion effect is dominant, while above $Z = 14$ radiative losses increase rapidly. Although the crossover point depends upon the particular criterion for Q reduction and is thus somewhat arbitrary, the model provides a convenient operational distinction between low Z and medium-high Z impurities in terms of their dominant effect on the fusion power gain. While it would be difficult to adopt the limit depicted in Fig. 2 as a strict design criterion, the model does serve as a useful method for comparing the effects of impurities of different Z on projected plasma performance.

III Limiter/Protective Plate Design

A. Configuration

The dominant thermal loads in TFTR will be incident upon the three primary structures shown in Fig. 3. The bumper limiter [6] is intended to absorb the major plasma heat load as well as perpendicular injection neutral beam heat loads due to incomplete ionization of the beam by the plasma. This limiter has a coverage of $\pm 60^{\circ}$ poloidally from the torus midplane and extends

around the entire toroidal circumference. The surface area is ~ 2 x 10^5 cm^2. It has not yet been decided whether to actively cool the bumper limiter or to use radiative cooling.

An array of moveable limiters is located in one toroidal position. These limiters are large, actively cooled plates with a total area of ~ 3 x 10^4 cm^2, each mounted on an actuator mechanism as shown. The moveable limiters, due to their small area, are not capable of absorbing the full plasma load for the entire pulse. They will be used in compression scenarios for short times.

The neutral beam shine-through for tangential injection will impinge upon protective plates located in the appropriate positions on the outer vessel circumference. These plates subtend a poloidal angle of ± 30° from the vessel midplane and also protect the vessel wall during faults when large neutral beam energy fluxes may be present. For these loads, radiative cooling is sufficient. Use of the plates as neutral beam calorimeters may require active cooling.

In addition to these three components, the vacuum vessel bellows assemblies are protected from direct plasma bombardment by bellows cover plates. These plates will be installed in those regions not covered by the bumper limiter or protective plates. They are not intended to take any major heat load.

A conceptual design of the bumper limiter is shown in Fig. 4. The construction of the moveable limiters and protective plates is similar. The first surface is comprised of tiles, nominally 10 cm x 10 cm, fabricated from among the candidate materials discussed in Section IV. These titles are attached to a backing plate made of stainless steel or Inconel depending upon the operating temperature and required strength. There will be twenty backing

plate segments around the torus, each of which has three sections covering the poloidal angles of -60° to -30°, -30° to $+30^{\circ}$, and $+30^{\circ}$ to $+60^{\circ}$. The individual backing plate/title assemblies must be capable of remote installation and removal.

The tiled structure affords a number of advantages. Thermal stresses are reduced (depending upon the details of the attachment) since the tiles are largely unrestrained. The backing plate will serve as a heat shield for the vacuum vessel if the limiter is radiatively cooled or can be actively cooled itself to prevent ratcheting of the tile temperature on successive pulses. Due to the relatively small tile size, the tile time constant for eddy current decay can be short enough for certain materials to significantly reduce the forces associated with plasma disruptions. This is discussed in Section III C. At present it is assumed that the replacement of individual damaged tiles would require removal of the particular backing plate/tile assembly; however, the tile construction would obviate the need of refabricating the entire first surface.

B. Thermal Loads

The plasma thermal load on the bumper limiter is calculated using a model[6] which assumes that heat flows along magnetic field lines and falls off exponentially from the outer magnetic surface with a characteristic scrape-off distance λ. From other calculations [7] the relevant range for λ is 0.4 cm to 2.5 cm. The associated plasma energy flux distributions are shown in Fig. 5 as functions of the poloidal angle. To be conservative, it is assumed that the total 33.5MW is incident on the limiter. The distribution is symmetric about the mid-plane where the flux goes to zero, since the plasma is assumed to be tangent to the bumper limiter at this point. Recent data from PLT[8] suggest that the energy flows across field lines as well. This would

increase the energy flux at the midplane and somewhat reduce the peak value from that calculated using the present model.

The anticipated neutral beam flux to the bumper limiter is shown in Fig. 5 also, and assumes that in normal operation a maximum of ~ 14% of the neutral beam power is transmitted through the plasma. This corresponds to average electron densities of $\langle n_e \rangle \sim 3 \times 10^{13} cm^{-3}$. The neutral beam flux to the protective plates (outer circumference) is similar to that in Fig. 5, except that at certain points, the overlap of two sources could double the power. The combined direct neutral beam energy flux and plasma energy flux for the bumper limiter is shown in Fig. 5, assuming 33.5MW total power and λ = 0.4 cm. This is used as a reference distribution as far as the peak flux is concerned, while the larger scrape-off result is used to estimate power to the larger poloidal angle region.

The peak energy flux to the moveable limiters has been estimated to be in the $3kW/cm^2$ - $5kW/cm^2$ range. As stated previously, it is for this reason that the moveable limiters will not be used for the entire 1.5s pulse. Using a 2-D finite element thermal transport code, Budny[9] has calculated the thermal response of a bumper limiter constructed of one of the candidate tile materials - TiC coated graphite (See Section IV) and a stainless steel backing plate. Fig. 6 shows the temperature evolution during a pulse for various surfaces of the tile and backing plate as indicated. The energy flux distribution used is similar to that of Fig. 5 for a total heat load of 33.5MW including a plasma load (λ = 0.4 cm) and neutral beam load. Fig. 6(a) shows the region of maximum tile temperature (~ 1850 C) while Fig. 6(b) shows the region of maximum backing plate temperature (~ 590 C). The limiter is radiatively cooled with the vacuum vessel temperature being 100 C. The cycle shown is in periodic equilibrium, i.e., the temperature just prior to each

successive pulse is constant. Since the TiC coating has a small thermal mass and thickness these results are generally applicable to graphite with other coatings.

For the elevated tile temperatures, sublimation may be a problem [10]. To estimate its effect, we can write that the average relative impurity concentration due to sublimation is given by

$$\frac{n_I}{\langle n_e \rangle} = k \frac{\Gamma A \tau_p}{V \langle n_e \rangle} , \qquad (5)$$

where Γ is the sublimation flux, A is the area of the sublimating surface, V is the plasma volume, τ_p is the the particle confinement time, and k is the fraction of the sublimation flux which enters the plasma. Solving Eq. 5 for Γ, taking $n_I/\langle n_e \rangle = 10^{-3}$ (as indicated in Fig. 2 for Ti, which is the dominant sublimation species), $V = 4.4 \times 10^7$ cm^3, $\tau_p = 0.05$s, $\langle n_e \rangle = 8 \times 10^{13}$ cm^{-3}, $k = 1$, and the high temperature area to be $\sim 10^4$ cm^2, we get that $\Gamma \sim 7 \times 10^{15}$ cm^{-2}sec^{-1} ($\sim 9 \times 10^{-3}$ Pa vapor pressure). In the case of TiC this corresponds to a temperature of $\sim$ 1830 C [11]. This is very close to the calculated peak temperature of 1850C. Considering tnat these calculations are conservative in assuming that all of the sublimated impurities enter the discharge and that the total 33.5MW heat load is incident on the limiter with a small λ, it is unlikely that sublimation will cause serious contamination in well behaved discharges.

The peak backing plate temperature during the pulse is $\sim$ 500C, which would result in a 20% decrease in the strength of stainless steel. This is considered further in Section III C.

Calculations [9] for the thermal evolution of copper cladded with vanadium (described in Section IV) show peak temperatures of $\sim$ 1300C which are

below the sublimation limit of 1400C for vanadium. This limit was calculated from Eq. 5 and the limits in Fig. 2, using similar assumptions to the TiC case. Backing plate temperatures are in the 500C range for this case also.

If the plasma undergoes a major disruption, the thermal energy will be rapidly deposited on the limiters, protective plates, and vessel walls. The maximum projected stored energy in the TFM mode is 16.5 MJ. For the reference disruption time constant of 200 μs, depending upon the area over which the energy is deposited, some surface melting of the tile materials being considered will occur [9].

C. Mechanical Loads

The dominant mechanical load of the limiters and protective plates occurs when the plasma undergoes a major disruption. The rapid plasma current decay and typical inward motion causes eddy currents to flow in the surrounding conductors, including the tiles and the backing plates. This is shown schematically in Fig. 7 for the tiles in the bumper limiter. The bumper limiter is most strongly affected by the disruption because of the expected inward motion of the plasma and the increased toroidal field strength. Because the flux surfaces of the plasma are not, in general, tangent to the tiles, eddy currents will flow around them as indicated. The maximum value of the eddy current in 24kA, assuming that the disruption time τ_D is much shorter than the eddy current decay time constant of the material τ_M [12]. With the 7.8 T toroidal field at the tile, the force/length on the tile is $\sim 1.9 \times 10^8$ dynes/cm. The maximum eddy current is reduced from this value as τ_D/τ_M increases. For $\tau_D/\tau_M = 1$, the current is reduced by 35%, and for $\tau_D/\tau_M \geq 10$, the reduction factor is $\sim (\tau_D/\tau_M)^{-1}$. For the graphite based tiles considered in Section IV, the reduction is significant, though the design of an appropriate tile attachment has not yet been completed. For Cu based tiles

very little reduction is realized due to the large electrical conductivity. The attachment of Cu based tiles is a formidable problem. In both cases, a dynamic load analysis is required to calculate the mechanical behavior of the tiles. Such calculations are in progress [13].

Calculations of the effect of eddy currents on the backing plate show that for the temperatures quoted in the calculations of Section III B, the strength of stainless steel is marginal [13]. Investigations are underway to determine whether the stainless steel backing plate can be stiffened sufficiently or whether Inconel or some other high strength material will be required.

IV Materials Studies

A. Candiate Materials

The materials being considered for tile fabrication are described in Table II. They include layered composites fabricated with substrates having good thermal characteristics (copper or graphite) and coatings or claddings which are intended to provide good surface properties. Although bare graphite has been used for limiters in some devices, in TFTR it would be operating at elevated temperatures such that chemical sputtering could be a problem [5]. Due to the stringent concentration limits shown in Fig. 2 for higher Z materials, nothing above V (Z = 23) has been considered for a tile front surface. This guideline thus precludes the use of bare copper (Z = 29).

Details of the coated materials in Table II have been given by Mattox [14], while those for the cladded materials have been given by Kaminsky [15], each of whom has coordinated the respective fabrication of samples for the TFM impurity control program. These samples have been subjected to a number of investigations at various laboratories to determine mechanical properties, surface properties, and hydrogen isotope retention properties as described in

the following sub-sections. The reference designations for the various materials from Table II will be used for convenience.

B. Mechanical Properties

Thermal fatigue and shock tests of candiate materials were performed by Ulrickson[11] using electron beam (EB) irradiation. In the fatigue tests, TiB_2/Cu, V/Cu, and Ti/Cu were subjected to 1 kW/cm^2 for 0.5s and 1000 pulses, while TiC/C was subjected to 1 kW/cm^2 for 1.5s and 5000 pulses. TiB_2/Cu showed spalling of the coating and Ti/Cu showed severed cracking. V/Cu exhibited only slight surface cracking while TiC showed just discoloration. The flux limits for EB pulse lengths of 0.5s and 1.5s are shown in Table III. These limits, which were set by the melting of respective coating/cladding surface or the substrate, afford a relative comparison of material behavior. Results of neutral beam irradiation are described in Ref. 11.

EB fatigue tests were also conducted by Whitley and Cowgill[16] with 1 kW/cm^2, 1.5s pulses using radiative cooling, and 2 kW/cm^2, 1.5s pulses with active cooling. After 200 cycles for both sets of conditions, the TiC/C system sustained the least damage, confirming the results of Ulrickson.

The shear strength of Ti/Cu and V/Cu were measured at room temperature and 300C [15]. In both cases, the shear strength of the bond exceeded that of the copper, which fractured.

On the basis of these bulk tests, TiC/C and V/Cu appear to be the most viable coating system and cladding system respectively. Relative to one

another the TiC/C has somewhat better bulk properties for the fluxes anticipated in TFTR; however, questions still remain as to whether the comparatively thin coating will adequately resist erosion due to the plasma environment.

As a preliminary test of this, a TiC/C limiter has been exposed to the PDX plasma [17]. The limiter has thus far been exposed during only one experimental run of ~ 30 discharges. During this period, it was moved into the discharge and was subjected to an energy deposition shown in Fig. 8 as a function of position. These energies were inferred from bulk temperature measurements using thermocouples. At the largest energies, the peak flux was ~ 0.5 kW/cm^2 for 0.5s. A scrape-off distance of 1.7 cm was determined from these data. No increase in either Ti or C contamination was seen, and the only changes observed on the limiter surface were two discolored spots ~ 3 mm in diameter. Coated limiters are also being studied on ISX [18,19].

The V/Cu system would be improved by using a thicker V cladding [17]. For the anticipated fluxes, the optimum thickness is ~ 2.3 mm. Since V is expensive and difficult to purchase in large quantities, an expolosion bonded combination of 0.5 mm V and 0.7 mm stainless can be used instead to give similar thermal properties. One other promising alternative is to use a V-Ti alloy such as V-10% Ti or V-20% Ti instead of pure V [15]. These alloys are more readily available and have higher ductility, which is an advantage in the explosion bond process. A test limiter for PDX is planned using the V-Ti alloy/SS/Cu combination.

C. Surface Properties

Low energy hydrogen erosion yields for some of the coatings and claddings have been measured, using a Kaufman ion source, by Mattox, et al.[20]. The hydrogen energy was in the range of 0.25 keV to 1.0 keV, characteristic of

plasma ions incident on the limiter. Some of these data are listed in Table IV. Kaminsky[21,22] has measured total deuterium sputtering yields for a range of deuterium energies from 1 keV to 60 keV, typical of unconfined neutral beam ions which strike the limiter. These rates were determined by Rutherford backscattering analysis of sputter deposits. Some of these data are reproduced in Table V.

In addition to these measurements, Roth, et al. [23], have studied low energy light ion sputtering for some of the materials considered here. From these data and those in Table V, the impurity production rates normalized by the total power to the limiter are plotted in Fig. 9 as functions of the incident deuterium energy. These rates are shown for TiC and Ti and, for comparison, C (physical sputtering only) and W. The deuterium is assumed to be mono-energetic. The particle current is calculated from the total power to be limiter assuming that the usual sheath conditions[24] prevail so that ~ 74% of the power is carried by the deuterium ions. Although the peak impurity production rate for TiC is a factor of 16 greater than that for W, the concentration limit for W (from Fig. 2) is only 1/40 times that for TiC. The actual rate will depend upon the energy of the impacting deuterium. Wampler, et al. [25] have measured this for PLT and find that it is > 500 eV, though not necessarily mono-energetic. At these energies, TiC compares even more favorably to W as far as impurity production rate.

In comparing the TiC rates to those of C, above 100 eV the C would appear better since its concentration limit is ~ 8 times that of Ti. However, at elevated temperatures, the C production rate can be a factor of 4-5 greater than that plotted [5].

Surface erosion rates are also plotted in Fig. 9, assuming a duty factor of one. The peak energy flux in the TFM is ~ 1 kW/cm^2. If we assume that

there are 2000 such pulses/year the duty factor is $\sim 10^{-4}$. The maximum yearly erosion for TiC would be $\sim$ 60 μm. This is approximately a factor of 2-3 larger than the typical coating thickness, suggesting that in those poloidal locations receiving the large heat flux, erosion of the thin coatings may be significant.

Outgassing rates have been measured for TiB_2/C, TiC/C, V/Cu, and 304LN stainless steel [15]. At room temperature the rates for the coatings and claddings are from 1-3 times greater than that for degreased 304LN stainless steel. Considering that these materials would cover only 20% to 30% of the vessel area, this is a tolerably low rate. At the higher temperatures these rates are significantly larger than that for 304LN.

D. Hydrogen Isotope Retention

The hydrogen isotope retention properties of the limiter materials are important in view of the tritium inventory limitations as well as their impact on recycling. Wilson and Pontau[26] have measured the deuterium trapping characteristics for a number of candidate materials using ion implantation with primarily gas re-emission analysis. Table VI is a compilation of their results for the saturation deuterium retention values as functions of implant temperatures immediately after implantation with 10 keV D_3^+ (3.3 keV/atom).

Ion implantation and nuclear profiling measurements of Wampler, et al. [27] show that for SiC, TiB_2, VB_2, B_4C, B, C, and Si, the implant H(D) is retained where it comes to rest in the near surface region up to saturation densities which are in agreement with the retention measurements of Wilson and Pontau [26].

Thermal release rates have also been measured for these materials by Wilson and Pontau[26] using thermal desorption techniques. Nuclear profiling

by Wampler, et al. [27] shows that the profiles are relatively unchanged during thermal release, suggesting that detrapping rather than bulk diffusion is the rate limiting process.

The behavior of the Ti and V claddings is dramatically different from the coatings in that after implantation the near surface region retains little of the implanted ions [27]. Since the overall retention is large, most of the ions appear to be diffusing into the bulk [26]. This accounts for the much greater retention for these materials as noted in Table VI.

For the coatings, in which essentially all implanted hydrogenic ions are retained in the near surface regions, Wampler, et al. [27] have shown that isotopic exchange can be used to reduce the concentration of a particular species. Fig. 10 shows typical isotopic exchange scenarios for B, TiC, VB_2 and TiB_2 with 3 keV implanted D being exchanged with 3 keV implanted H. These data are in excellent agreement with theory as shown.

To consider the implications of these measurements for TFTR we note that the limiter tiles, if radiatively cooled, will operate in the 300C to 500C temperature range. Based upon the anticipated energy flux to the limiter and PLT measurements, the D/T ion fluence per pulse will be $\sim 10^{18} cm^{-2}$. Even at the elevated temperatures, the retention for Ti is extremely high and has not reached saturation at $10^{18} cm^{-2}$ fluence as noted in Table VI. V, however, will reach saturation above ~ 300C within a few pulses. The retained tritium in V, assuming a limiter area of $2 \times 10^5 cm^2$ and equal D/T densities, is ~ 2.5 kCi at ~ 300C and 1 kCi at ~ 500C, just after implantation. Significant thermal desorption should occur above 350C. These retention values can be reduced by an order of magnitude by pack boriding the surface as shown in Table VI for the VB_2/V/Cu case.

Among the coatings, TiB_2 has the lowest retention (500 Ci at ~ 500C) while TiC is lower than V by a factor of two.

E. Summary of Materials Studies

On the basis of all of the data, TiC/C appears to be the best coating system. The salient problem associated with its use in TFTR is the predicted erosion lifetime and the possibility that arcing or disruption heat loads will seriously damage the coating. Further tests in PDX should provide additional information on this. The hydrogenic retention properties are satisfactory.

Among the claddings, those with a V first surface performed the best. For the reasons mentioned in Section IV B, the V/SS/Cu system seems optimum. Since this combination will have the same thickness V as the samples tested for hydrogenic retention, the results quoted in Section III D indicate that at the higher temperatures, characteristic of TFM operations, the tritium retention for this system would be a factor of 2-3 worse than for TiC. This is still within an acceptable range, however. If this system is pack borided to produce a VB_2/V/SS/Cu combination, the retention would be reduced by an order of magnitude; however, the erosion of the VB_2 would have to be considered. As mentioned in Section IV B, consideration is being given to substituting a V-Ti alloy for pure V; however, the retention characteristics for this would need to be investigated. Tests of one or more of the V systems as a PDX limiter material will be undertaken in the near future. One other major problem with any system using a Cu substrate is the large eddy current force discussed in Section III C.

V Gettering

One technique which has been used successfully in a number of tokamaks to control impurities is gettering [5] by evaporating Ti on the vacuum vessel

walls. A summary of gettering procedures and results is given by Dylla [4]. Besides controlling impurities, gettering also reduces the hydrogenic species recycling [28], a feature which was particulary important to the high powered neutral beam heating experiments on PLT [29]. In this case, gettering reduced the large density rise which would otherwise accompany the neutral injection. This facilitated the attainment of high ion temperatures and associated penetration into the collisionless transport regime.

Control of the density during neutral injection is also important to the operation of TFTR. In addition, it is necessary to control the deuterium-tritium density ratio to optimize Q for the particular mode of operation. Gettering, in conjunction with selected gas puffing or pellet injection, can provide such control.

The salient problem with gettering in TFTR is that large quantities of tritium will be absorbed. The maximum allowable absorbed quantity will be ultimately determined from on-site meteorological data; however, it is unlikely to be more than the gas load equivalent of 50-100 machine pulses. It is thus necessary to regenerate or desorb the stored tritium from the getter at comparatively frequent intervals. One additional problem confronting a getter design is the plasma radiative heat load, which may be up to 33 W/cm^2 for the 1.5s pulse. The following sub-sections discuss the research and engineering efforts which are underway within the TFM impurity control program towards developing a suitable gettering system for TFTR.

A. Ti Sublimation

As mentioned previously, Ti sublimation has been used in a number of tokamak devices. Malinowski[30] has investigated the decomposition of deuterided Ti films. He showed that the deuterium can be desorbed from the films in reasonable times at 250C even in the presence of some impurities such

as C and O. Fig. 11 shows his measured decomposition rate for a 908Å film at 250C as a function of deuterium loading. The rate is high for D/Ti > 1.5 corresponding to a deuteride phase. For .1 < D/Ti < 1.5, the rate is constant in a mixed phase including deuterium in dilute solution and precipitated deuterides. At low concentrations (D/Ti < .1) the rate follows Sieverts law and goes to zero at D/Ti = 0. The reason why significant thermal desorption required much higher temperatures in the data of Wilson and Pontau[26] (See Section IV D.) is that for their much thicker bulk samples the D concentration was always small (D/Ti < 4×10^{-4}) with a corresponding slow desorption rate at 250C.

The design of a Ti sublimation gettering system has been discussed by Sredniawski.[31] It consists of two actuator mechanisms which are mounted on flanges at the vacuum vessel midplane. These actuators stroke Ti sublimation sources to the center of the vessel where they evaporate Ti (with suitable shields) onto removable panels on the top and bottom of the vacuum vessel. The total coverage is ~ 10% of the vessel area, and the estimated D_2 pumping speed is 3×10^4 l/s. The panels are actively cooled to maintain their temperature below 100C during machine operation, and are heated to 250C-300C to desorb tritium.

A number of problems remain, however. Titanium may be desorbed from a panel by the plasma and redeposited on the vacuum vessel wall, causing increased tritium absorption there. The vessel is capable of being heated to 250C which should be sufficient to desorb such films; however, this bake out requires substantial time to carry out to avoid large temperature gradients on the vessel. If large layers of titanium are built up on the plates, flaking may be a problem. Finally, the system would require a number of diagnostic ports and is, in general, quite complicated.

B. Zr/Al Bulk Getter

The Zr/Al alloy ST101 (84% Zr; 16% Al by weight) is a getter which reversibly absorbs hydrogenic species while chemisorbing impurities such as C, N, and O [32]. It operates at 200C - 400C where the impurity chemisorption into the bulk is sufficiently rapid to permit good hydrogenic pumping. To regenerate the stored hydrogenic species, the temperature is increased to 600C -700C to increase the hydrogen equilibrium pressure. This high temperature also serves to activate the pump after air exposures, which cause the surface to be saturated by impurities.

A Zr/Al system conceptual design for TFTR is shown in Fig. 12 and described by Sredniawski [31]. The Zr/Al modules are in the form of corrugated strips with the Zr/Al bonded to a constantan substrate, and are heated resistively [32]. Arrays of these modules are located in the bellows regions as shown, thus having minimal impact on diagnostics. The coverage is 9% of the vessel area and the D_2 pumping speed is 5.4×10^5 l/s. The elevated operating temperature obviates the need for active cooling. The thermal load on the vacuum vessel during regeneration is substantial, however, and local gradients may be problematic. The lifetime of the getters due to the impurity saturation limit is approximately one year of TFTR operation. The fatigue lifetime due to repeated regeneration has been measured to be longer than that determined by impurity saturation [33].

Although the plasma will not be in direct contact with the getters, the high Z of Zr (40) is cause for concern in consideration of the limit in Fig. 2. Arrays are presently being fabricated for installation in PDX to investigate this problem as well as determine how these getters operate in a tokamak environment.

In the present design, the getters would require four to eight hours of regeneration after one day of operation [31]. One possible scenario which would eliminate the necessity of such frequent regeneration is to operate them at a temperature intermediate between normal operation and regeneration. Because the duty factor of TFTR will be small (1.5s pulse with a 300s interval) a quasi-steady state will be reached, where the quantity of absorbed gas from the 1.5s pulse will be desorbed in the interval between pulses [34]. This is shown in Fig. 13. The quantity $q_n(t_p)/Q$ is the amount of gas absorbed in units of equivalent gas loads per pulse and is plotted as a function of the number of pulses n for 550C and 600C operation. The equilibrium loadings q_e/Q are the equivalent of ~ 52 pulses (550C) and ~ 29 pulses (600C).

C. Advanced Concepts

Mendelsohn and Gruen[35] have shown the alloys of Zr/V/Fe will absorb and regenerate hydrogenic species similar to Zr/Al but at lower temperatures. In particular, the alloy $ZrV_{1.6}Fe_{0.4}$ will operate at 200C (which is still high enough not to require active cooling in TFTR) and regenerate at 450C-500C, which would substantially reduce the thermal loading on the vacuum vessel. There are also preliminary indications that such alloys can be bonded to suitable substrates and pump impurities as effectively as Zr/Al at the same temperature [33].

VI Discussion

Since the control of impurities is likely to remain a major problem for tokamaks for some time, it is important to consider the relevance of the TFM impurity control effort to future devices. The large area axisymmetric limiter concept and related materials studies are directly applicable to the next generation of machines after TFTR. The anticipated energy fluxes for

both limiters and divertor plates are similar to those considered for TFTR/TFM [36]. If coatings are to be used in high duty factor devices, some methods for in-situ deposition will be necessary. The pulse length in the future tokamaks will be much longer and this will require active cooling. However, if this requirement is adequately considered in the design of future vacuum vessels, it can be accommodated much more easily than it can in TFTR where only limited space is available.

The work on the forces and thermal loads due to disruptions is also of general applicability. The operation of TFTR itself will provide important information on these problems.

It is clear that gettering as discussed in Section V is not directly applicable to long pulse devices. It is important to recognize, however, that TFTR is intended to investigate a number of plasma physics questions concerning confinement properties in high temperature collisionless regimes. To the extent that gettering facilitates this, it is crucial to the following generation of machines. It would also be useful to determine the importance of recycling control to various modes of beam heated plasma operation. A divertor may provide the necessary control of both impurities and recycling; however, it substantially complicates tokamak operation. Other schemes should be investigated, including a hot liner [5], which may reduce impurities and hydrogenic recycling and would be compatible with long pulse operation.

VII Acknowledgments

It is a pleasure to acknowledge a number of useful discussions with R. Budny, S. Cohen, F. Dylla, M. Kaminsky, R. Little, M. Malinowski, D. Mattox, M. Mendlesohn, K. Owens, J. Schmidt, C. Singer, J. Sredniawski, M. Ulrickson, W. Wampler, and K. Wilson. This work was supported by the U. S. Department of Energy Contract No. DE-AC02-76-CH03073.

References

[1] Princeton University, Princeton, NJ (1976) unpublished.

[2] TFTR Improvements Project Scoping Study Report, R. Little, ed., Report PPPL-1480, Princeton Plasma Physics Laboratory, Princeton University, Princeton, NJ (1978) unpublished.

[3] C. E. Singer, TFTR Physics Group Report #22, Plasma Physics Laboratory, Princeton University, Princeton, NJ (1980) unpublished.

[4] H. F. Dylla, 4th International Conference on Plasma Surface Interactions in Controlled Fusion Devices (Garmisch-Partenkirchen, F.R.G., 21-25 April 1980) paper R.5.

[5] G. M. McCracken and P. E. Stott, Nucl. Fus. 19 (1979) 889.

[6] J. A. Schmidt, Comments on Plasma Physics and Controlled Fusion V (1980).

[7] C. E. Singer, F. G. P. Seidl, J. M. Ogden, and R. J. Hawryluk, TFTR Physics Group Report #21, Princeton University, Plama Physics Laboratory, Princeton, NJ (1980) unpublished.

[8] S. A. Cohen, R. Budny, G. M. McCracken, and M. Ulrickson, to be published.

[9] R. Budny, 4th International Conference on Plasma Surface Interactions in Controlled Fusion Devices (Garmisch-Partenkirchen, F.R.G., 21-25 April 1980) paper J.7.

[10] R. Behrisch, Nucl. Fus. 12 (1972) 695.

[11] M. Ulrickson, US-Japan Workshop on Divertors, Impurity Control, and First Walls (Tokai, Japan, 17-20 March 1980) to be published.

[12] D. Weissenburger and U. Christensen, Report PPPL-1517, Plasma Physics Laboratory, Princeton University, Princeton, NJ (1979) unpublished.

[13] J. Bialek, Private Communication.

[14] D. M. Mattox, Journal of Thin Solid Films 63 (1979) 213.

[15] M. Kaminsky, International Conference on Metallurgical Coatings (San Diego, California, 21-25 April 1980) paper RE.3, to be published in Journal of Thin Solid Films.

[16] J. B. Whitley and D. F. Cowgill, International Conference on Metallurgical Coatings (San Diego, California, 21-25 April 1980) Paper Re.3 to be published in Journal of Thin Solid Films.

[17] M. Ulrickson and J. Cecchi, International Conference on Metallurgical Coatings (San Diego, California, 21-25 April 1980) paper RE.8, to be published in Journal of Thin Solid Films.

[18] R. A. Langley, L. C. Emerson, A. W. Mullendore, and J. B. Whitley, 4th International Conference on Plasma Surface Interactions in Controlled Fusion Devices (Garmisch-Partenkirchen, F.R.G., 21-25 April 1980) paper K.4.

[19] J. B. Whitley and A. W. Mullendore, International Conference on Metallurgical Coatings (San Diego, California, 21-25 April 1980) paper RE.1, to be published in Journal of Thin Solid Films.

[20] D. M. Mattox, A. W. Mullendore, H. O. Pierson, and D. J. Sharp, J. Nucl. Mater. 85&86 (1979) 1127.

[21] M. Kaminsky, to be published in J. Nucl. Mater.

[22] M. Kaminsky, S. K. Lam, and K. Moy, to be published in the Journal of Thin Solid Films.

[23] J. Roth, J. Bohdansky, and A. P. Martinelli, International Conference on Ion Beam Modification of Materials, J. Gyulai, T. Lohner, and E. Pasztor, eds., (Central Res. Inst. for Physics, Budapest, 1979) 1541.

[24] R. H. Lovberg, in Plasma Diagnostic Techniques, Huddlestone and Leonard, eds. (Academic Press, New York, 1965) 98ff.

[25] W. R. Wampler, S. T. Picraux, D. Brice, S. A. Cohen, H. F. Dylla, D. K. Owens, S. M. Rossnagel, G. M. McCracken, and C. W. Magee, submitted to Phys. Rev. Lett.

[26] K. W. Wilson and A. E. Pontau, 4th International Conference on Plasma Surface Interactions in Controlled Fusion Devices (Garmisch-Partenkirchen, F.R.G., 21-25 April 1980) paper H.5.

[27] W. R. Wampler, B. L. Doyle, D. K. Brice, and S. T. Picraux, Sandia Laboratories Internal Report (1980).

[28] E. S. Marmar, J. Nucl. Mater. 76&77 (1978) 59.

[29] H. Eubank, et al., Seventh International Conference on Controlled Nuclear Fusion, 1978, 1 (Vienna, International Atomic Energy Agency, 1979).

[30] M. E. Malinowski, J. Nucl. Mater. 85&86 (1979) 957.

[31] J. Sredniawski, 8th Symposium on Engineering Problems of Fusion Research (San Francisco, California, 13-16 November 1979) to be published in Proceedings.

[32] B. Ferrario and L. Rosai, Proceedings 7th International Congr. & 3rd International Conf. Solid Surfaces (Vienna, 1977) 359.

[33] B. Ferrario, Private Communication.

[34] J. L. Cecchi, S. A. Cohen, and J. J. Sredniawski, J. Vac. Sci. and Tech. 17 (1980).

[35] M. H. Mendelson and D. M. Gruen, International Symposium on the Properties and Applications of Metal Hydrides (Colorado Springs, Colorado, 7-11 April 1980) to be published in J. Less-Common Metals.

[36] U. S. Contribution to the International Tokamak Reactor Workshop, 1979, INTOR.

TABLE I. BALDUR CODE SIMULATION FOR TFTR [3]

INPUT PARAMETERS	
Plasma Major Radius (m)	2.48
Plasma Minor Radius (m)	0.85
Toroidal Field on Axis (T)	5.2
Neutral Beam Power (MW)	33.5
Plasma Current (MA)	2.5
Impurity Concentration (cm^{-3})	0.0
PROJECTED PLASMA PARAMETERS AFTER 1.5s. NEUTRAL BEAM HEATING	
Average Electron Density (cm^{-3})	8×10^{13}
Peak Electron Temperature (keV)	14
Peak Ion Temperature (keV)	22
Plasma Pressure/Magnetic Field Pressure, β	0.03
Fusion Power Gain, Q	2.5

TABLE II. CANDIDATE MATERIALS

SAMPLE MATERIALS		Fabrication[2]	Reference Designation
coating/ cladding (thickness)	Substrate[1]		
TiB_2 (~30 μm)	POCO Graphite	CVD	TiB_2/C
TiB_2 (~100 μm)	Cu	PS	TiB_2/Cu
TiC (~20 μm)	POCO Graphite	CVD	TiC/C
B (~20 μm)	POCO Graphite	CVD	B/C
VB_2 (~20 μm)/V(0.5mm)	Cu	PB/ExBd[3]	VB_2/V/Cu
V (0.5 mm)	Cu	ExBd	V/Cu
V(0.5 mm)/Mo (1.5 mm)	Cu	ExBd/ExBd[4]	V/Mo/Cu
V(0.5 mm)/Nb (3.2 mm)	Cu	ExBd/ExBd[4]	V/Nb/Cu
V-20% Ti alloy (0.5 mm)	Cu	ExBd	V-Ti/Cu
V (0.5 mm)/SS(0.7 mm)	Cu	ExBd/ExBd[4]	V/SS/Cu
Ti (0.5 mm)	Cu	ExBd	Ti/C

Notes:

[1]Substrate thickness for thermal tests and tiles is 1.27 cm. Thinner samples used for some surface and retention measurements.

[2]Coating Methods: CVD-chemical vapor deposition
PS-plasma spray
PB-pack boriding

Cladding Method: ExBd-Explosion Bond.

[3]Combination of 0.5mm V explosion bonded to Cu with the V surface pack borided.

[4]Triple material combination - two explosion bonds.

TABLE III. THERMAL SHOCK TEST RESULTS [11]

Sample	Thermal Flux Limit (kW/cm^2)	
	0.5s Pulse	1.5s Pulse
TiC/C	4.0	2.45
TiB_2/C	2.5	1.45
B/C	2.6	1.7
V/Cu	5.0	2.4
V/Mo/Cu	5.0	3.0
VB_2/V/Cu	5.0	2.4
Ti/Cu	4.1	2.5
TiB_2/Cu	5.0	2.45

TABLE IV. LOW ENERGY HYDROGEN EROSION YIELDS (ATOMS/ION) [20]

Sample	Hydrogen Energy (keV)		
	.25	.5	1
TiB_2	9.0×10^{-4}	5.0×10^{-3}	1.0×10^{-2}
TiC	1.4×10^{-3}	3.4×10^{-3}	9.4×10^{-3}
V	5.0×10^{-4}		

TABLE V. TOTAL DEUTERIUM SPUTTERING YIELDS (ATOMS/ION) [21, 22]

Sample	Deuterium Energy (keV)				
	1	5	10	40	60
TiB_2	1.4×10^{-2}	5.2×10^{-3}	3.3×10^{-3}	1.4×10^{-3}	9×10^{-4}
Ti	1.1×10^{-2}	5.0×10^{-3}	3.1×10^{-3}	1.3×10^{-3}	9×10^{-4}
V	1.0×10^{-2}	4.9×10^{-3}	3.0×10^{-2}	1.1×10^{-3}	8×10^{-4}

TABLE VI. SATURATION DEUTERIUM RETENTION (D/cm^2) AS A FUNCTION OF IMPLANT TEMPERATURE IMMEDIATELY AFTER IMPLANTATION WITH 10 keV D_3^+ (3.3 keV/atom) [26]

Sample	SAMPLE TEMPERATURE		
	102C	302C	502C
TiB_2/C	2×10^{17}	1×10^{17}	2×10^{16}
TiB_2/Cu	3×10^{17}	- - - -	- - - -
VB_2/V/Cu	2×10^{17}	1×10^{17}	3×10^{16}
TiC/C	4×10^{17}	2×10^{17}	1×10^{17}
Ti/Cu	$> 10^{19}$	$> 10^{18}$	$\gtrsim 5 \times 10^{17}$
V/Cu	$> 10^{19}$	6×10^{17}	2×10^{17}

Figure Captions

Fig. 1 The Tokamak Fusion Test Reactor.

Fig. 2 Impurity concentration limits as functions of impurity atomic number Z. Limits correspond to $\lesssim$ 10% reduction in Q due to β reduction and depletion of deuterium and tritium as shown.

Fig. 3 Diagram of the limiters and protective plates in TFTR. The bumper limiter covers the entire toroidal circumference. The protective plates are located in areas irradiated by the neutral beams.

Fig. 4 Bumper limiter conceptual design showing tiles mounted on a solid backing plate. Construction of the moveable limiters and protective plates is similar.

Fig. 5 Calculated plasma and neutral beam energy fluxes incident on the bumper limiter. The total power is indicated for each case along with the assumed scrape off distance, λ, for the plasma fluxes.

Fig. 6 (a) Calculated evolution of TiC-graphite tile and stainless steel backing plate for 33.5MW plasma plus neutral beam heat load as shown in Fig. 5. The temperatures for four surfaces are shown: (1) TiC front surface, (2) graphite back surface, (3) stainless steel front surface, and (4) stainless steel back surface. The poloidal location is that where the highest tile temperature is reached.

(b) Same as (a) except that the poloidal location is that where the highest backing plate temperatures are reached.[9]

Fig. 7 Eddy currents and resulting force/length for a tile. The eddy current I_{ec} is calculated from a disruptive scenario where the plasma current decreases as the plasma moves inward. it is assumed that the disruption time τ_D is small compared to the eddy currents decay time constant τ_M.

Fig. 8 Energy deposition on a TiC/C test limiter in PDX as a function of limiter minor radius. A scrape off distance of 1.7 cm was inferred from these data.[17]

Fig. 9 Impurity production rate normalized by the total power to the limiter as a function of the incident deuterium energy. This is plotted for C, TiC, Ti, and W. The erosion rate normalized by the energy flux to the limiter is shown also, assuming a duty factor of unity.

Fig. 10 Isotopic exchange measurements for B, TiC, VB_2, and TiB_2. Deuterium ions were implanted to the fluences indicated followed by hydrogen implantation. Predictions of the TRIM code are shown.[27]

Fig. 11 Decomposition rate of deuterided titanium film as a function of the deuterium/tritium concentration ratio.[30]

Fig. 12 Conceptual design for a Zr/Al getter system on TFTR. The getter modules are corrugated strips which are combined in arrays and mounted in the bellows regions of the torus.[31]

Fig. 13 Calculated scenarios for Zr/Al transient getter operation. The quantity $q_n(t_p)/Q$ is the getter gas loading in units of equivalent machine pulses. This is plotted as a function of the number of pulses for 550C and 600C operation. The quantity q_e/Q is the equilibrium loading.[34]

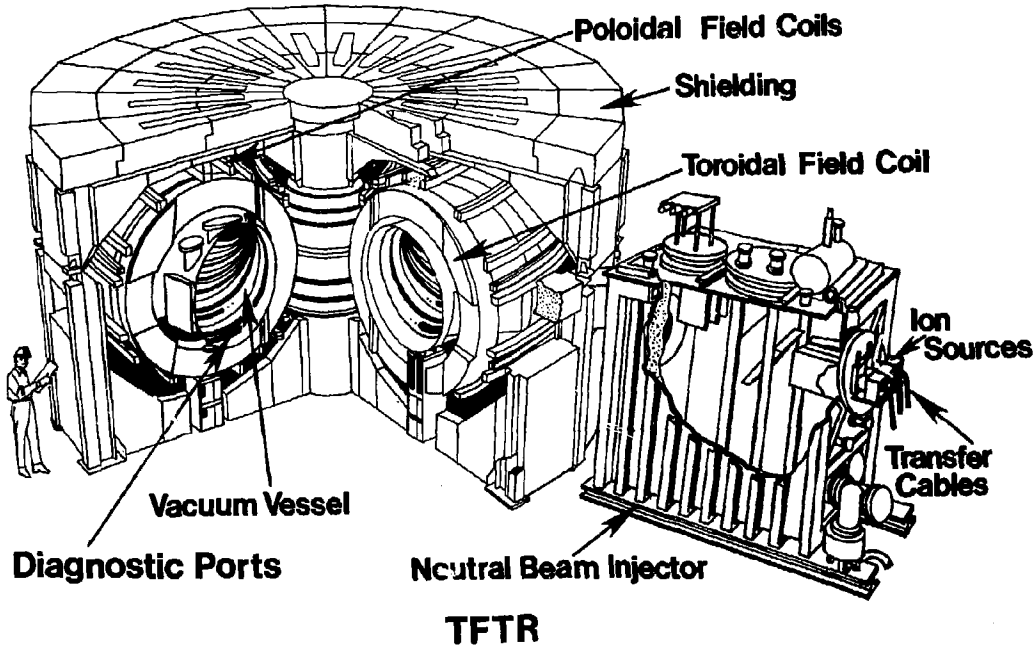

Fig. 1. (PPPL-784800)

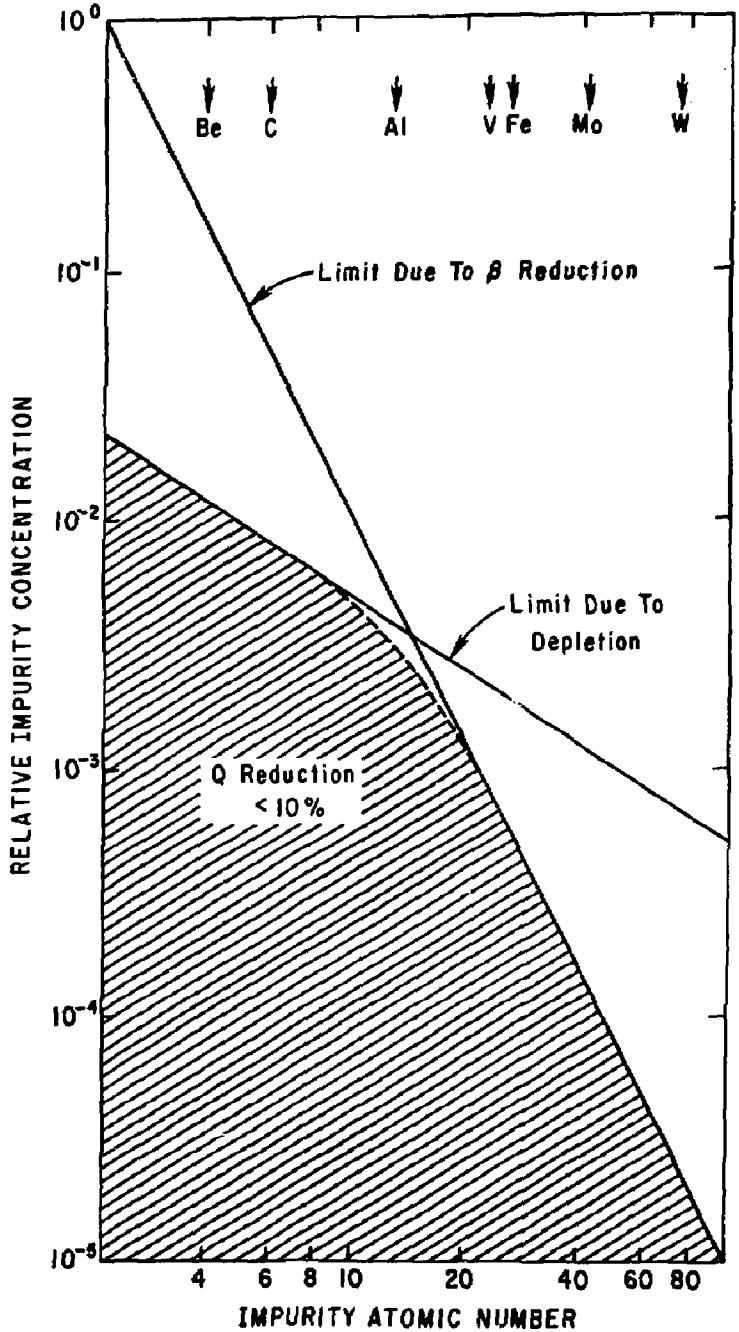

Fig. 2. (PPPL-803569)

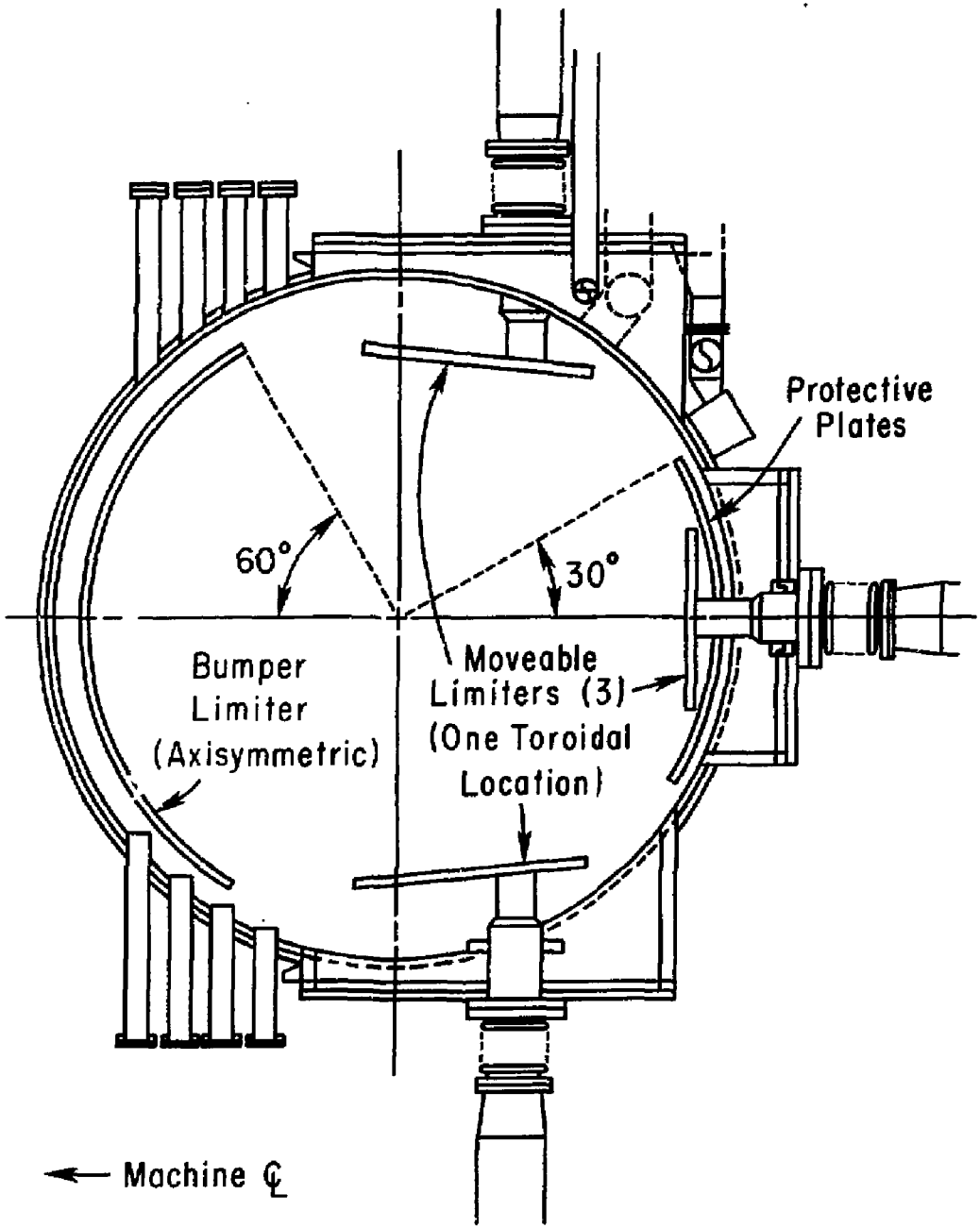

Fig. 3. (PPPL-803696)

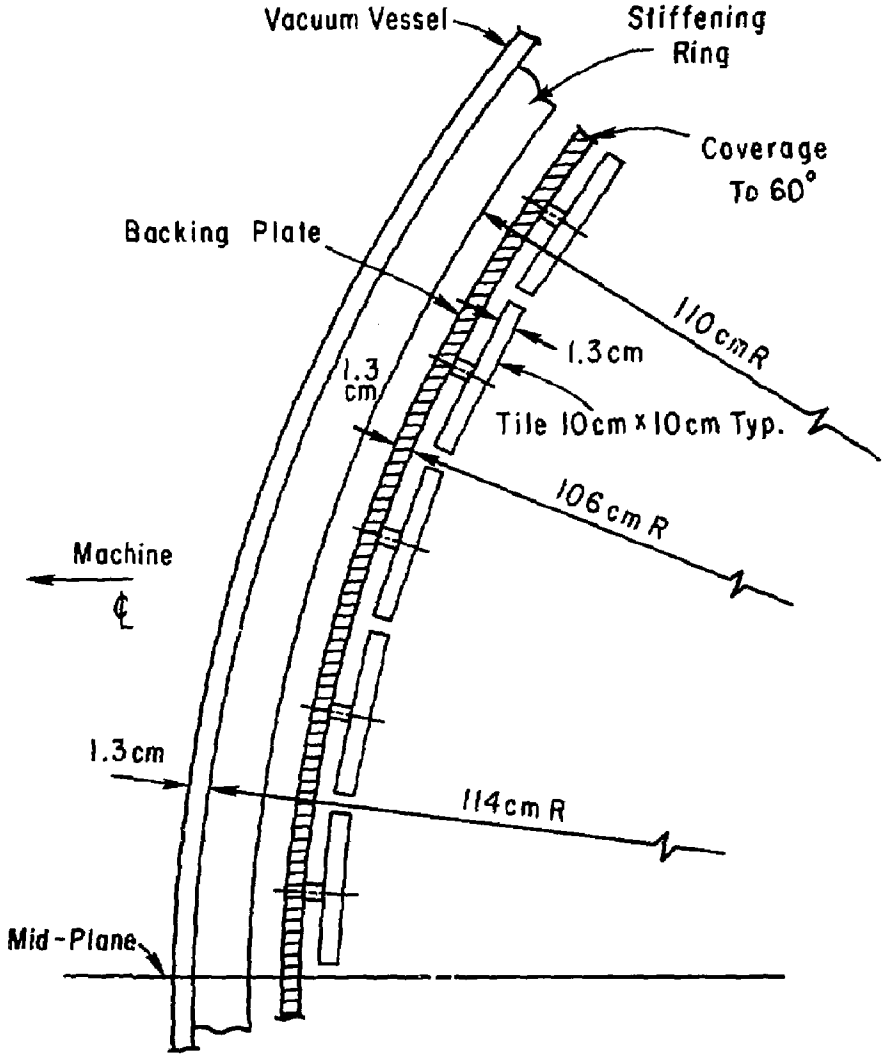

Fig. 4. (PPPL-803695)

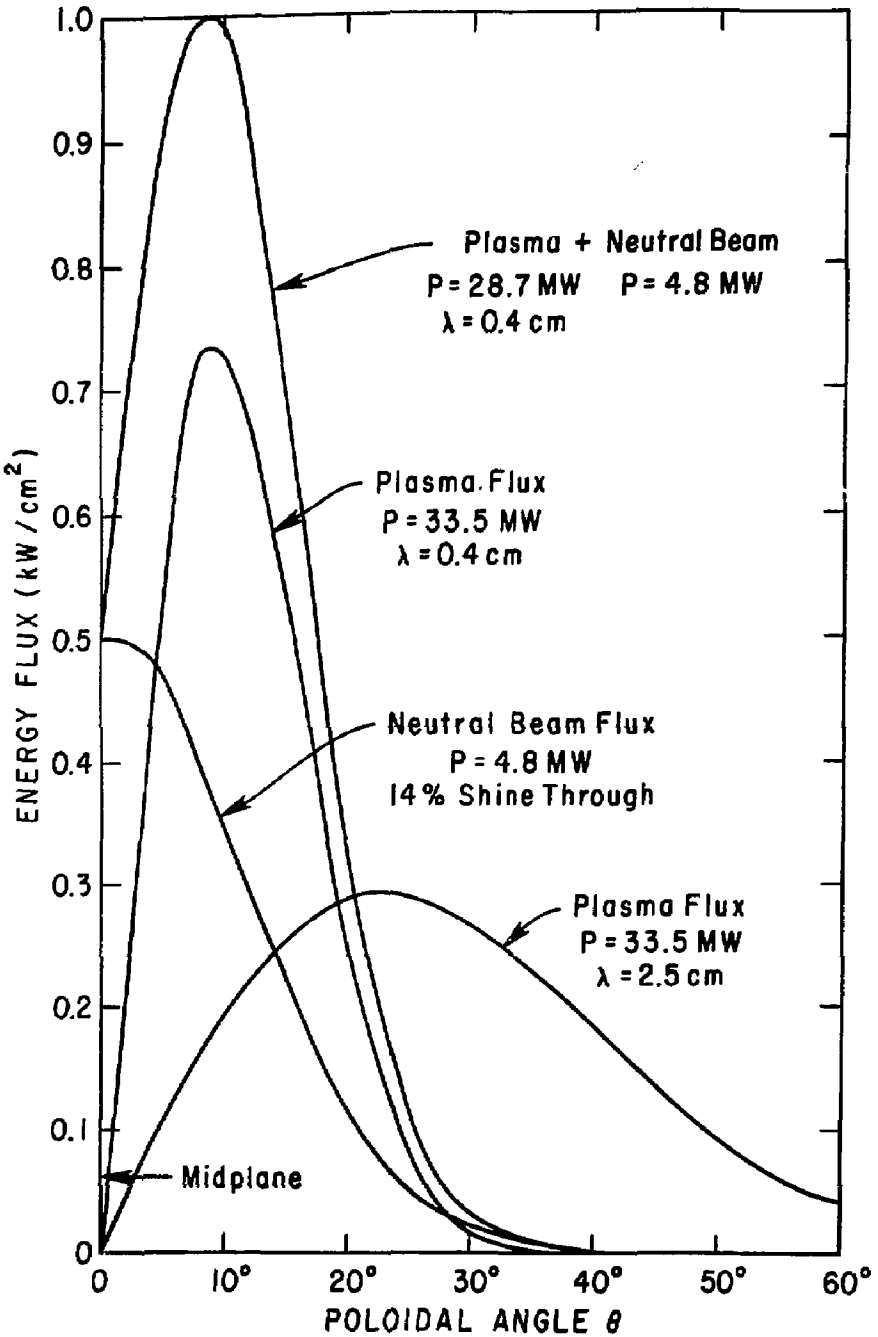

Fig. 5. (PPPL-803566)

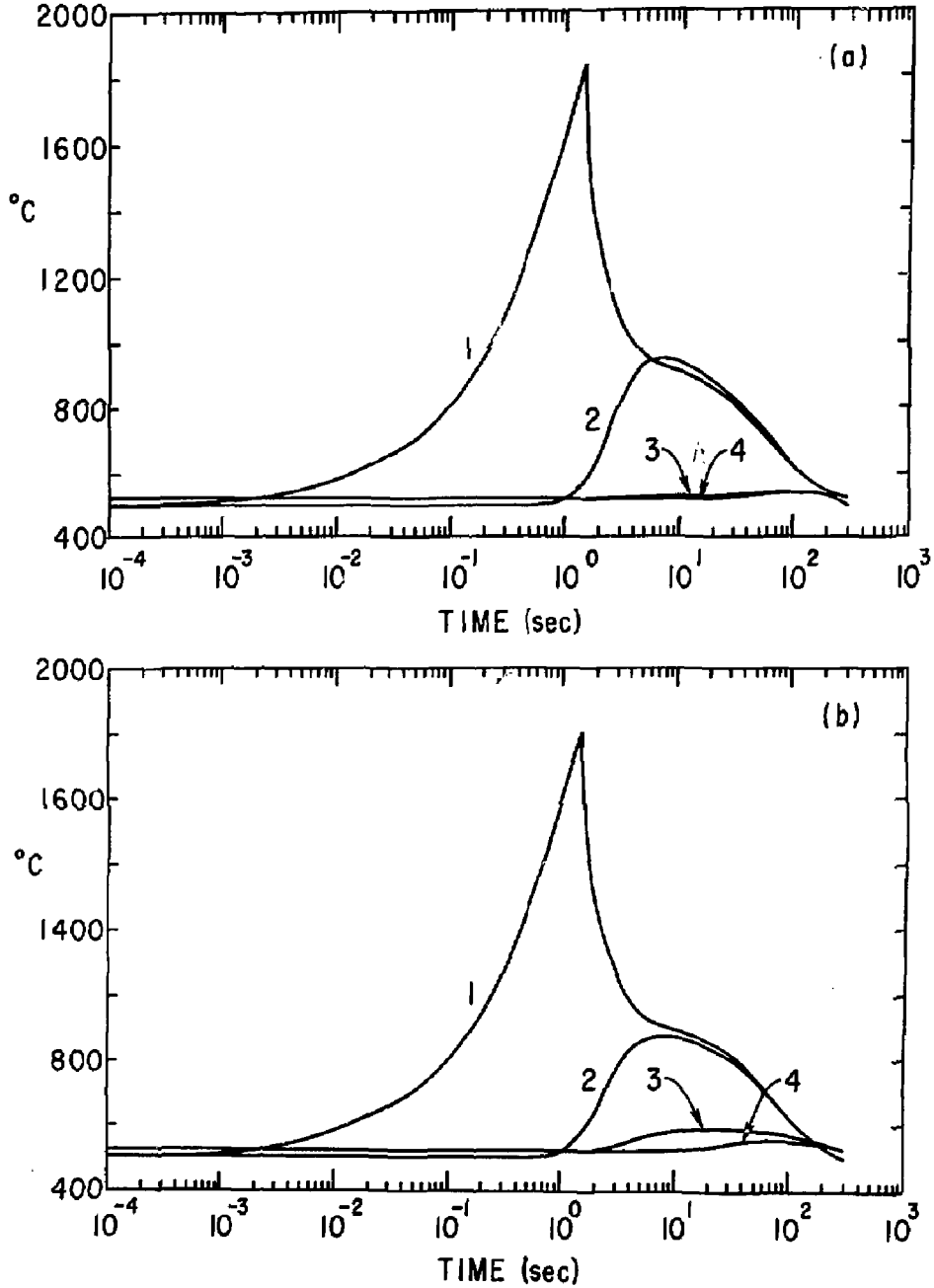

Fig. 6. (PPPL-803400)

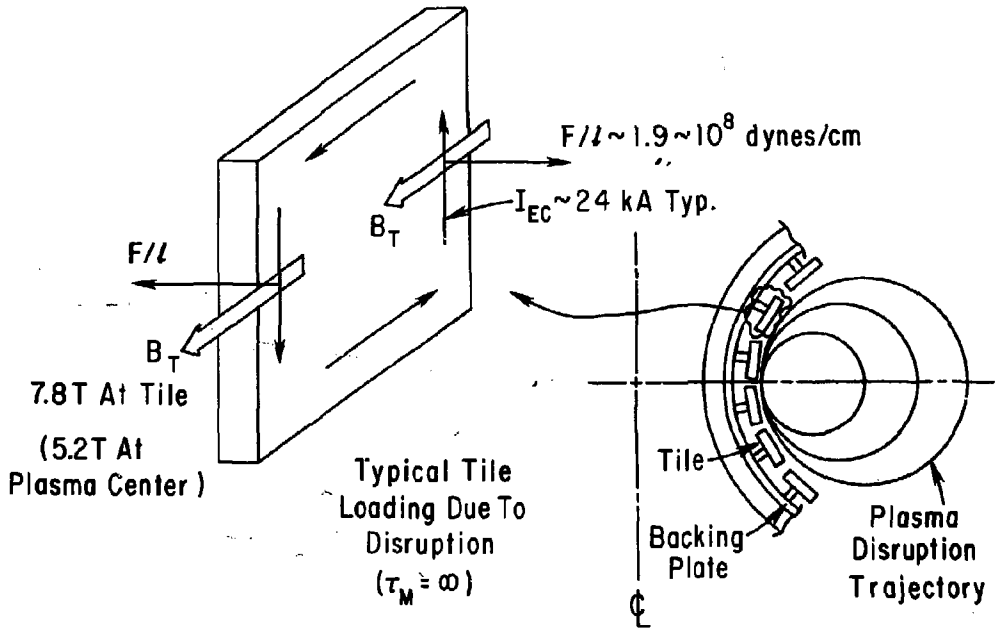

Fig. 7. (PPPL-803564)

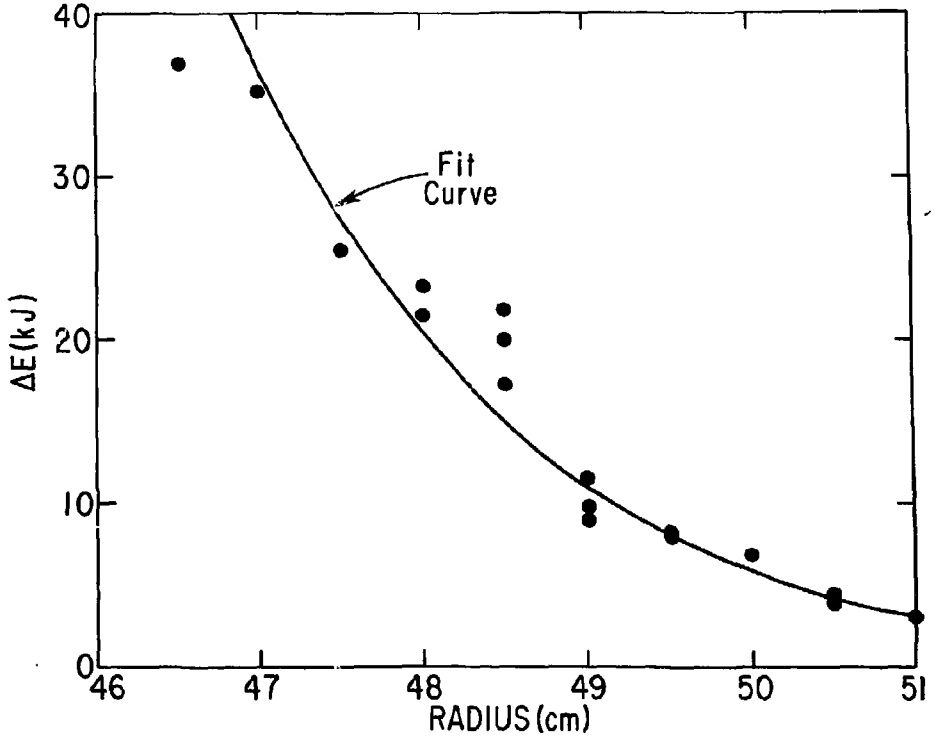

Fig. 8. (PPPL-603260)

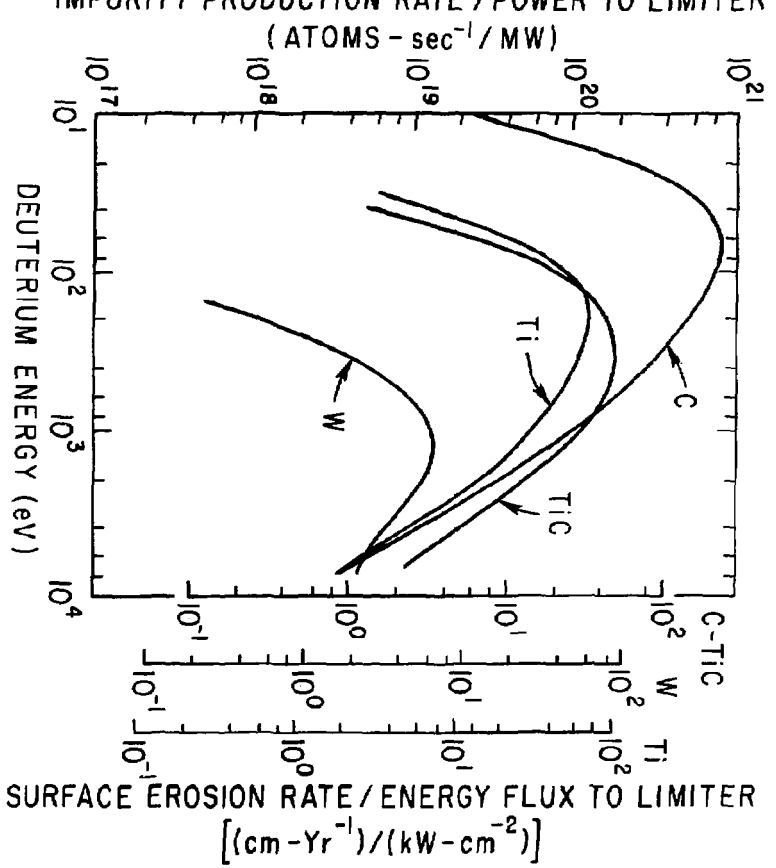

Fig. 9. (PPPL-803563)

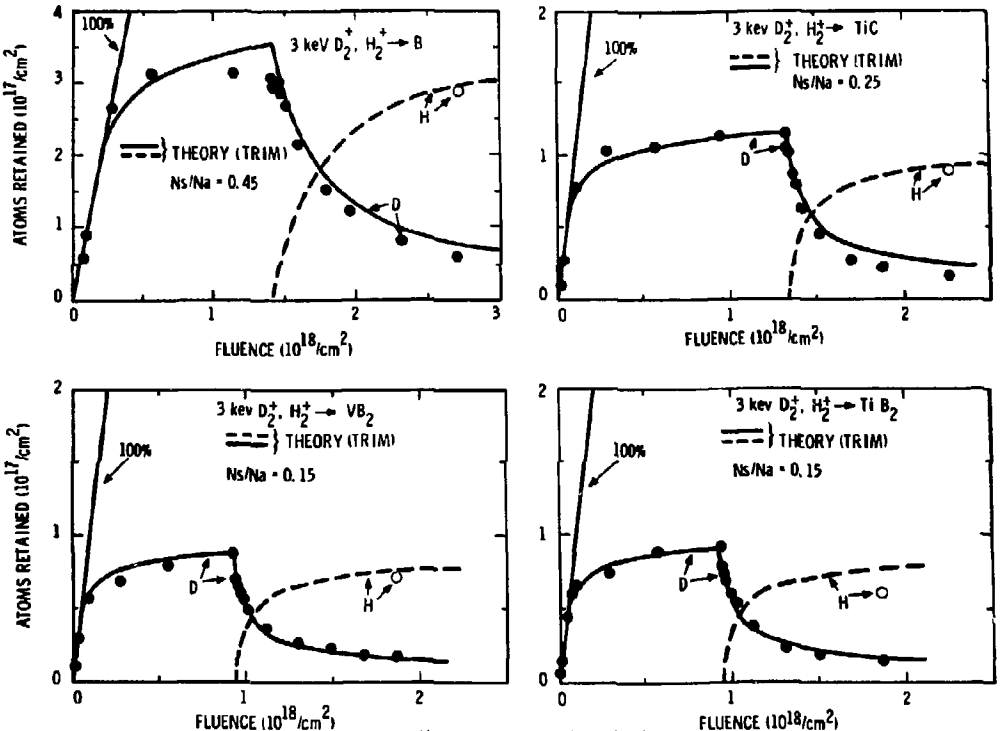

Fig. 10. (PPPL (4-9-80))

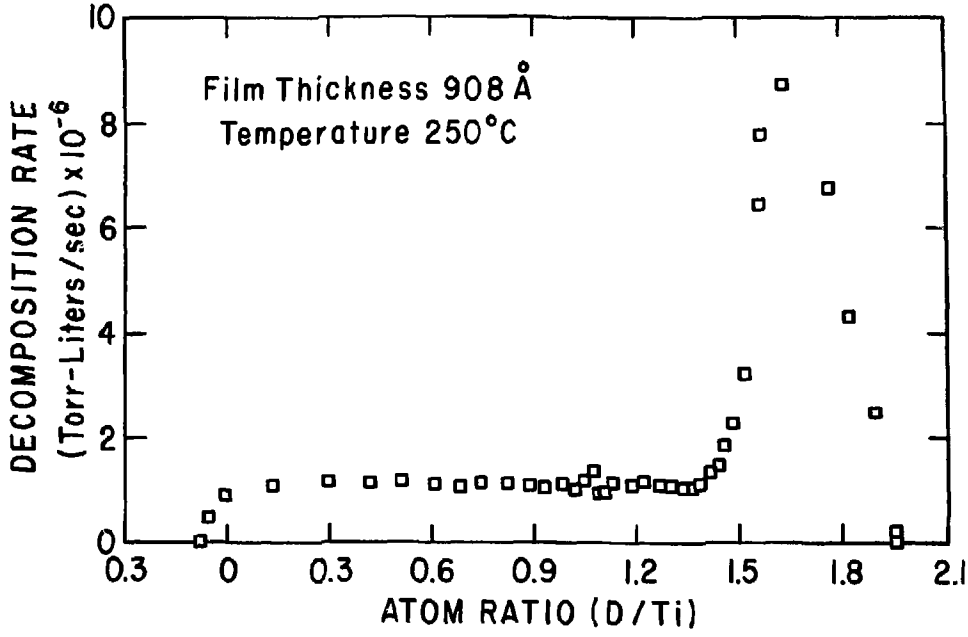

Fig. 11. (PPPL-803697)

SURFACE PUMPING ARRANGEMENT
Zr/Al GETTERING

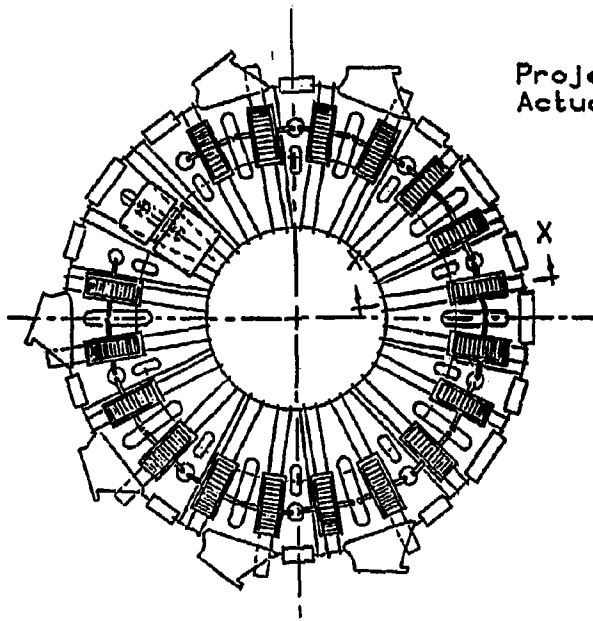

PLAN VIEW

Projected coverage=8.7%
Actual capture area
=95188cm^2

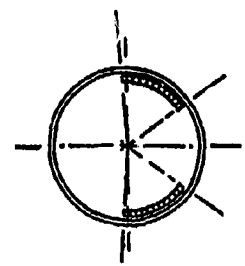

VIEW X-X

Fig. 12. (PPPL (4-9-80))

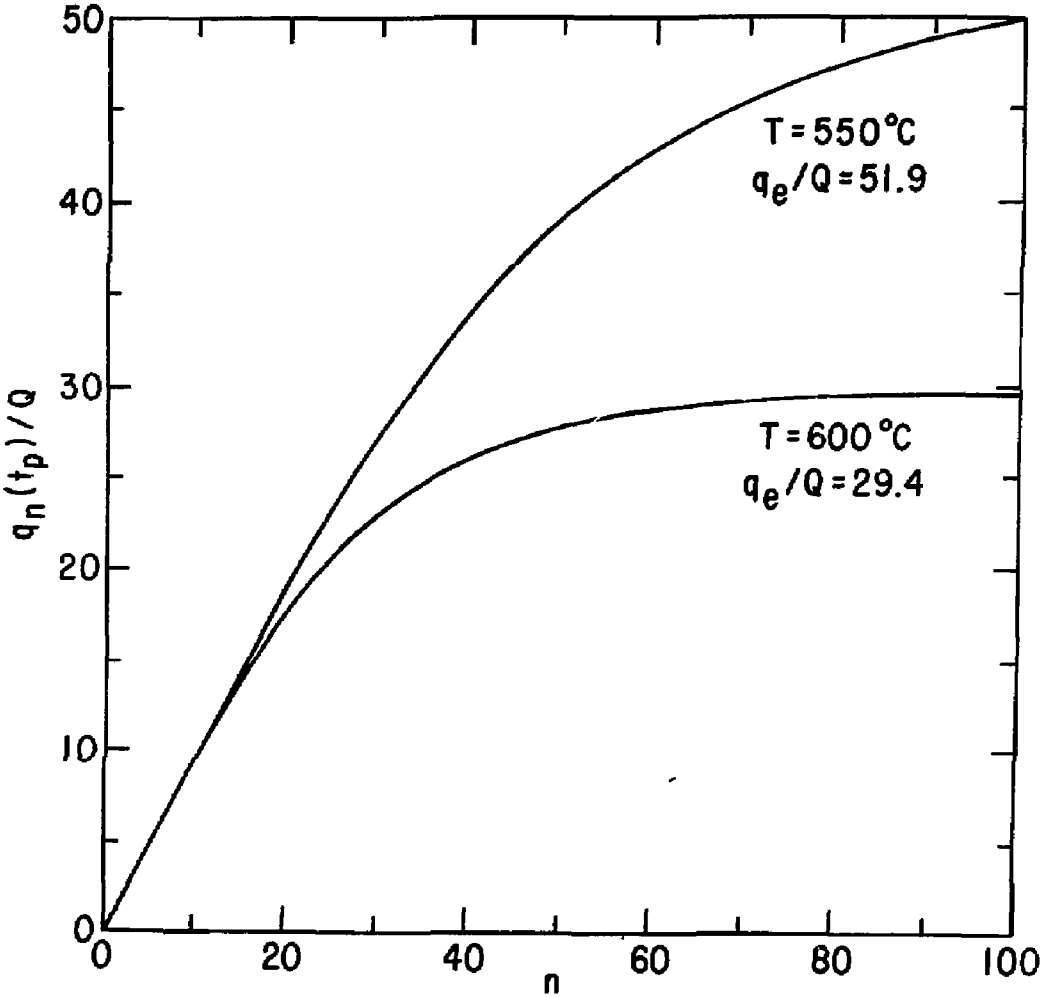

Fig. 13. (PPPL-803567)